Effect of Polystyrene-*b*-poly(ethylene oxide) on Self-Assembly of Polystyrene-*b*-poly(*N*-isopropylacrylamide) in Aqueous Solution

XIAODONG YE,[1] JINGYI FEI,[1*] KUI XU,[2] RUKE BAI[2]

[1]Department of Chemical Physics, University of Science and Technology of China, Hefei, Anhui 230026, China

[2]Department of Polymer Science and Engineering, University of Science and Technology of China, Hefei, Anhui 230026, China

Received 6 January 2010; revised 27 February 2010; accepted 3 March 2010
DOI: 10.1002/polb.22006
Published online in Wiley InterScience (www.interscience.wiley.com).

ABSTRACT: Mixed micelles of polystyrene-*b*-poly(*N*-isopropylacrylamide) (PS-*b*-PNIPAM) and two polystyrene-*b*-poly(ethylene oxide) diblock copolymers (PS-*b*-PEO) with different chain lengths of polystyrene in aqueous solution were prepared by adding the tetrahydrofuran solutions dropwise into an excess of water. The formation and stabilization of the resultant mixed micelles were characterized by using a combination of static and dynamic light scattering. Increasing the initial concentration of PS-*b*-PEO in THF led to a decrease in the size and the weight average molar mass ($\langle M_w \rangle$) of the mixed micelles when the initial concentration of PS-*b*-PNIPAM was kept as 1×10^{-3} g/mL. The PS-*b*-PEO with shorter PS block has a more pronounced effect on the change of the size and $\langle M_w \rangle$ than that with longer PS block. The number of PS-*b*-PNIPAM in each mixed micelle decreased with the addition of PS-*b*-PEO. The average hydrodynamic radius $\langle R_h \rangle$ and average radius of gyration $\langle R_g \rangle$ of pure PS-*b*-PNIPAM and mixed micelles gradually decreased with the increase in the temperature. Both the pure micelles and mixed micelles were stable in the temperature range of 18 °C–39 °C. © 2010 Wiley Periodicals, Inc. J Polym Sci Part B: Polym Phys 48: 1168–1174, 2010

KEYWORDS: atom transfer radical polymerization (ATRP); core-shell polymers; diblock copolymers; dynamic light scattering; poly(*N*-isopropylacrylamide); polystyrene

INTRODUCTION Polystyrene-*b*-poly(ethylene oxide) (PS-*b*-PEO) is an important amphiphilic diblock copolymer because of its properties as steric stabilizers for latex particles[1,2] and its potential applications in areas such as drug delivery.[3] The micelles of PS-*b*-PEO in aqueous solution have been investigated by laser light scattering,[4–6] fluorescence spectroscopy,[7–10] and electron microscopy.[11–13] The results show that PS-*b*-PEO copolymers may form micelles in water because water is a good solvent for PEO block and a nonsolvent for PS block. So far, not only the pure PS-*b*-PEO micelles but also mixed micelles of PS-*b*-PEO and surfactants have been studied.[14–16] Mixed micelles are so important because they have much more attractive properties than the pure micelles formed by individual surfactant or block copolymer, such as new structure or function can be easily achieved by simply change of the composition, rather than through synthesis of new surfactants or block copolymers. For example, Bronstein and coworkers have studied the comicellization of PS-*b*-PEO with cationic surfactant, cetylpyridinium chloride (CPC), and anionic surfactant, SDS.[14,15] They found such hybrid systems can be used to stabilize Pd, Pt, and Rh nanoparticles.[16]

Besides mixed micelles including pluronic surfactants,[17,18] until now mixed micelles containing diblock copolymers with one thermally sensitive block have received less attention. Pispas and his coworkers investigated the self-assembly behavior of mixed solutions consisting of poly(isoprene-*b*-ethylene oxide) (IEO) copolymer micelles and vesicle-forming didodecyldimethylammonium bromide (DDAB) and found there were two populations of nanoassemblies in the solutions, namely, block copolymer modified surfactant vesicles (BCMSVs) and surfactant-modified block copolymer micelles (SMBCMs).[19] It is quite interesting to find that BCMSVs and SMBCMs are both thermosenstive. Recently, Pispas and coworkers reported the thermo-induced aggregation behavior of poly(ethylene oxide)-*b*-poly(*N*-isopropylacrylamide) block copolymer in the presence of cationic surfactants.[20]

On the other hand, diblock copolymer with one hydrophobic block and one thermally sensitive block have received much attention.[21–26] Among the thermosensitive polymers studied, poly(*N*-isopropylacrylamide) (PNIPAM) with a lower critical solution temperature (LCST) at ~32 °C has been extensively used.[27,28] Tenhu and coworkers have studied the micellization behavior of series of amphiphilic diblock copolymers comprising PNIPAM as a thermosensitive block with hydrophobic blocks, either polystyrene or poly(*tert*-butyl methacrylate).[23] Zhang et al. have investigated the self-assembly

*Present address: Department of Chemistry, Columbia University, New York, NY 10027.
Correspondence to: X. Ye (E-mail: xdye@ustc.edu.cn)
Journal of Polymer Science: Part B: Polymer Physics, Vol. 48, 1168–1174 (2010) © 2010 Wiley Periodicals, Inc.

of polystyrene-*b*-poly(*N*-isopropylacrylamide) (PS-*b*-PNIPAM) with different block lengths in aqueous solutions[25] and the adsorption of the formed micelles or vesicles on a gold surface.[26] In this article, we study the effect of PS-*b*-PEO on the micellar formation of PS-*b*-PNIPAM and the stabilization of the resultant mixed micelles in aqueous solutions by a combination of static and dynamic laser light scattering. Our objective is to understand the effect of hydrophilic–hydrophobic ratio on the formation and stabilization of the mixed micelles.

EXPERIMENTAL

Materials

Poly(ethylene oxide) (PEO) capped with a methyl group at one end and a hydroxyl group at the other (M_n = 5000 g/mol, Fluka) was dried by azeotropic distillation in toluene before use. CuBr was purified by stirring in acetic acid, washing with methanol, and then dried *in vacuo*. Styrene was passed through a column of neutral alumina to remove inhibitor. Monomer *N*-isopropylacrylamide was recrystallized three times in a benzene/*n*-hexane mixture. Tetrahydrofuran (THF) was distilled over potassium under dry nitrogen atmosphere before use. 4,4′-Azobis(isobutyronitrile) (AIBN) was recrystallized from ethanol. Other chemicals were used as received. Poly(styrene)-*b*-poly(*N*-isopropylacrylamide) was prepared by reversible addition-fragmentation chain transfer polymerization, the details can be found elsewhere.[23,25,29–31] Briefly, styrene, AIBN, and chains transfer agent dithiobenzoate were added into a glass tube. After three freeze-vacuum-thaw cycles, the tube was sealed under vacuum and then placed in a thermostated bath at 68 °C for 24 h. The PS terminated with dithiobenzoate (PS-PhC(S)S) was precipitated into ethanol, filtered, and then dried in a vacuum oven at 40 °C. PS-PhC(S)S, NIPAM, AIBN, and THF were added into a glass tube. After three freeze-vacuum-thaw cycles, the tube was sealed under vacuum and then placed in a thermostate at 68 °C for 16 h. The polymer was precipitated into petroleum ether (bp 30–60 °C). Precipitation was repeated three times and the diblock copolymer was dried at 40 °C in a vacuum oven for 24 h. Two poly(styrene)-*b*-poly(ethylene oxide) diblock copolymers were synthesized by atom transfer radical polymerization following a procedure in ref. 32. PEO-Br macroinitiator was prepared by esterification of the PEO—OH with 2-bromoisobutyryl bromide. The atom transfer radical polymerization (ATRP) of styrene initiated by PEO—Br/CuBr in THF resulted in the PS-*b*-PEO diblock copolymer. The number average molecular weight (M_n) and the polydispersity (M_w/M_n) of diblock copolymers were characterized by a combination of gel permeation chromatography (GPC) and ^{1}H NMR spectra. GPC measurements were carried out on a Waters 150C using a series of monodisperse polystyrenes as the calibration standard and THF as the eluent with a flow rate of 1.0 mL/min. ^{1}H NMR spectra were measured on a Bruker DMX-500 NMR spectrometer using chloroform-*d* ($CDCl_3$) as the solvent and tetramethylsilane (TMS) as the internal standard. Here, we designate a block copolymer as A_m-*b*-B_n with the subscript m and n denoting the number of the units in A and B blocks. For PS_{207}-*b*-$PNIPAM_{357}$, PS_{108}-*b*-PEO_{114}, and PS_{313}-*b*-PEO_{114}, we have M_w/M_n = 1.17, 1.10, and 1.18.

Preparation of Micelles

Because both PS-*b*-PEO and PS-*b*-PNIPAM cannot be directly dissolved in water, a microphase inversion process was used to prepare the pure micelles and the mixed micelles.[33–35] The self-assembly of PS-*b*-PEO and PS-*b*-PNIPAM was induced by adding a 0.4 mL solution of PS-*b*-PEO and PS-*b*-PNIPAM in THF with the initial concentration of PS-*b*-PNIPAM $C_{\text{PS-}b\text{-PNIPAM}} = 1 \times 10^{-3}$ g/mL and different concentrations of PS-*b*-PEO dropwise into 40 mL of deionized water under stirring at 20 °C. As expected, THF quickly mixed with water. The water insoluble PS blocks of PS-*b*-PEO and PS-*b*-PNIPAM collapsed and aggregated to form a core, whereas the water-soluble PNIPAM blocks and PEO blocks form a protective shell. The small amount of THF introduced in the preparation was removed under a reduced pressure. The pure PS-*b*-PEO or PS-*b*-PNIPAM micelles were prepared by the same method in the same condition.

Laser Light Scattering

A spectrometer (ALV/DLS/SLS-5022F) equipped with a multi-τ digital time correlator (ALV5000) and a cylindrical 22 mW UNIPHASE He-Ne laser (λ_0 = 632.8 nm) as the light source was used. In static LLS,[36,37] we were able to obtain the weight-average molar mass (M_w) and the z-average root-mean square radius of gyration ($(\langle R_g^2\rangle^{1/2}$) or written as $\langle R_g\rangle$) in a very dilute solution from the angular dependence of the excess absolute scattering intensity.

$$\frac{KC}{R_{vv}(q)} \approx \frac{1}{M_w}\left(1 + \frac{1}{3}\left\langle R_g^2\right\rangle_z q^2\right) \quad (C \to 0) \tag{1}$$

where $K = 4\pi^2(dn/dC)^2/(N_A\lambda_0^4)$ and $q = (4\pi n/\lambda_0)\sin(\theta/2)$ with C, dn/dC, N_A, and λ_0 being concentration of the polymer, the specific refractive index increment, the Avogadro's number, and the wavelength of light, respectively. The refractive index increments of the polymeric aggregates were calculated using an addition method.[38] In this study, the concentration is so low that the extrapolation to infinite dilution was not necessary. In dynamic LLS,[39] the intensity–intensity time correlation $G^{(2)}(t, q)$ in the self-beating mode is measured. $G^{(2)}(t, q)$ can be related to the normalized electric field–field time correlation function $g^{(1)}(t, q)$ as follows:

$$G^{(2)}(t,q) = \langle 1(t,q)1(0,q)\rangle = A[1 + \beta|g^{(1)}(t,q)|^2] \tag{2}$$

where A is the baseline; β is a parameter depending on the coherence of the detection, t is the delay time. $g^{(1)}(q, t)$ can be related to the characteristic line-width distribution $G(\Gamma)$ by the following:

$$g^{(1)}(q,t) = \int_0^\infty G(\Gamma)e^{-\Gamma t}d\Gamma \tag{3}$$

By using the CONTIN program developed by Provercher,[40,41] the Laplace inversion can be related to a line-width

distribution $G(\Gamma)$. For a pure diffusive relaxation, Γ is related to the translational diffusion coefficient D by $\Gamma/q^2 = D$ at $q \rightarrow 0$ and $C \rightarrow 0$, or a hydrodynamic radius $R_h = k_B T/(6\pi\eta D)$ with k_B, T, and η being the Boltzman constant, absolute temperature, and solvent viscosity, respectively. Therefore, $G(\Gamma)$ can be converted to a hydrodynamic radius distribution $f(R_h)$. All the solutions were clarified with a 0.45-μm PTFE Millipore filter.

RESULTS AND DISCUSSION

Because THF is a good solvent for the three blocks (PS, PEO, and PNIPAM), PS-*b*-PEO and PS-*b*-PNIPAM diblock copolymers were molecularly dissolved in THF. When the mixture of PS-*b*-PEO and PS-*b*-PNIPAM in THF was added dropwise into excess water, because THF is miscible with water, the diffusion of THF into water resulted in the interchain association of the PS blocks and the mixed micelles were formed. Pure micelles are formed when THF solution only contains PS-*b*-PEO or PS-*b*-PNIPAM diblock copolymers. By using this method, Wu and his coworkers have prepared a series of core-shell nanoparticles.[33–35] Figure 1 shows the initial PS-*b*-PEO concentration dependence on the size of pure PS-*b*-PEO micelles and mixed micelles of PS-*b*-PEO and PS-*b*-PNIPAM. The results reveal that the average hydrodynamic radius $\langle R_h \rangle$ and the average radius of gyration $\langle R_g \rangle$ of the pure

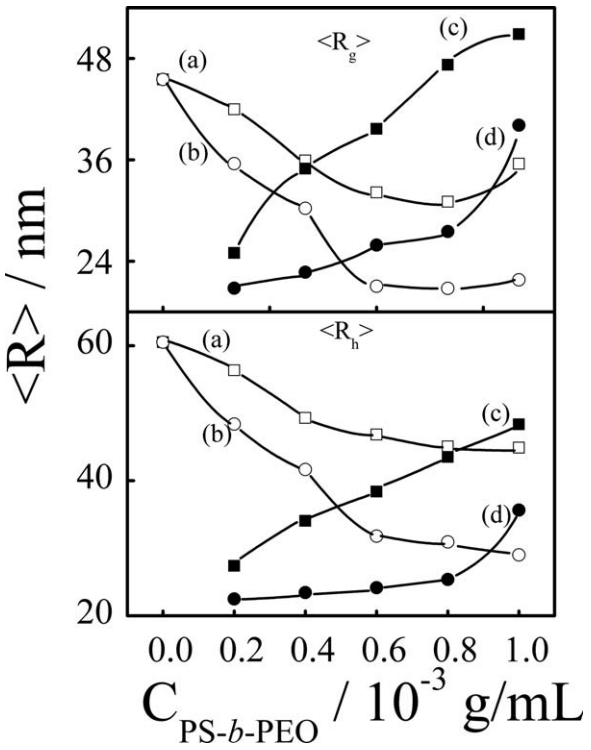

FIGURE 1 Initial PS-*b*-PEO concentration dependence on the average hydrodynamic radius ($\langle R_h \rangle$) and the average radius of gyration ($\langle R_g \rangle$) of the mixed micelles of PS-*b*-PEO and PS-*b*-PNIPAM or the pure micelles of PS-*b*-PEO. (a) PS-*b*-PNIPAM ($C = 1 \times 10^{-3}$ g/mL) + PS_{313}-*b*-PEO_{114}; (b) PS-*b*-PNIPAM ($C = 1 \times 10^{-3}$ g/mL) + PS_{108}-*b*-PEO_{114}; (c) PS_{313}-*b*-PEO_{114} without PS-*b*-PNIPAM; and (d) PS_{108}-*b*-PEO_{114} without PS-*b*-PNIPAM.

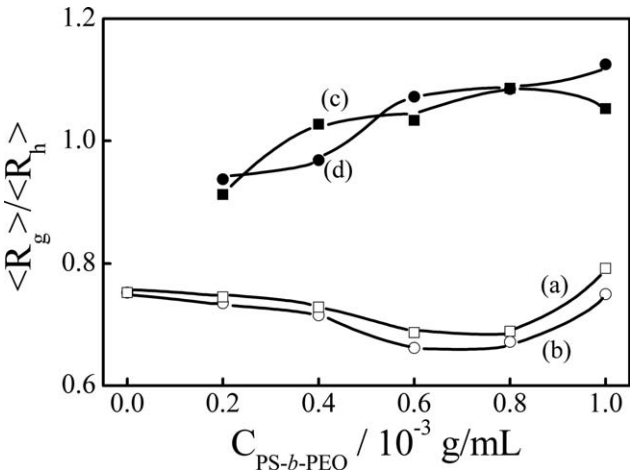

FIGURE 2 Initial PS-*b*-PEO concentration dependence on the ratio of average radius of gyration ($\langle R_g \rangle$) to average hydrodynamic radius ($\langle R_h \rangle$) of the mixed micelles of PS-*b*-PEO and PS-*b*-PNIPAM or the pure micelles of PS-*b*-PEO, where all symbols have the same meanings as in Figure 1.

PS-*b*-PEO micelles increased with the concentration. These trends are consistent with the results reported by Zhao et al., which are due to the increase in the interchain association with the initial concentration.[33] Figure 1 also shows that both $\langle R_h \rangle$ and $\langle R_g \rangle$ of the resultant mixed micelles decreased with the initial concentration of PS-*b*-PEO ($C_{PS\text{-}b\text{-}PEO}$) when $C_{PS\text{-}b\text{-}PEO}$ $\langle 6 \times 10^{-4}$ g/mL and $C_{PS\text{-}b\text{-}PNIPAM} = 1 \times 10^{-3}$ g/mL. Then, $\langle R_h \rangle$ and $\langle R_g \rangle$ leveled off with the further increase in $C_{PS\text{-}b\text{-}PEO}$. The PS_{108}-*b*-PEO_{114} has larger effect on the change of the size than PS_{313}-*b*-PEO_{114}. Note that the $\langle R_h \rangle$ and $\langle R_g \rangle$ of the aggregates prepared by Zhang et al. is larger than the size of pure PS-*b*-PNIPAM micelles in our experiments by using the same diblock copolymer, which maybe due to the different preparation methods and different ratios of water to THF solution.[25]

Figure 2 illustrates that the plots of $\langle R_g \rangle/\langle R_h \rangle$ versus the initial concentration of the PS-*b*-PEO. The ratio $\langle R_g \rangle/\langle R_h \rangle$ can reflect the structure of a polymer or a sphere. For uniform and nondraining sphere, hyperbranched cluster or micelle, and linear flexible random chain in a good solvent, $\langle R_g \rangle/\langle R_h \rangle$ is $\sim$0.774, 0.8–1.2, and 1.5–1.8.[42] For pure PS-*b*-PEO micelles, $\langle R_g \rangle/\langle R_h \rangle$ is in the range of 0.91–1.13, indicating PS-*b*-PEO micelles are core-shell structure with PEO as corona and polystyrene as core. $\langle R_g \rangle/\langle R_h \rangle$ increases with the concentration of PS-*b*-PEO, which is because $\langle R_g \rangle$ increases faster than $\langle R_h \rangle$. For pure PS-*b*-PNIPAM micelles, $\langle R_g \rangle/\langle R_h \rangle$ is 0.75, indicating that pure PS-*b*-PNIPAM micelles are uniform nondraining spheres. In comparison with PS-*b*-PNIPAM, the weight ratio of PS to PEO of the two PS-*b*-PEO diblock copolymers is higher than the weight ratio of PS to PNIPAM. So with the addition of PS-*b*-PEO, PS-*b*-PNIPAM diblock copolymers are replaced by PS-*b*-PEO in the mixed micelles, $\langle R_g \rangle/\langle R_h \rangle$ decreases due to higher density of core compared with the periphery. $\langle R_g \rangle/\langle R_h \rangle$ increases when $C_{PS\text{-}b\text{-}PEO} = 1 \times$

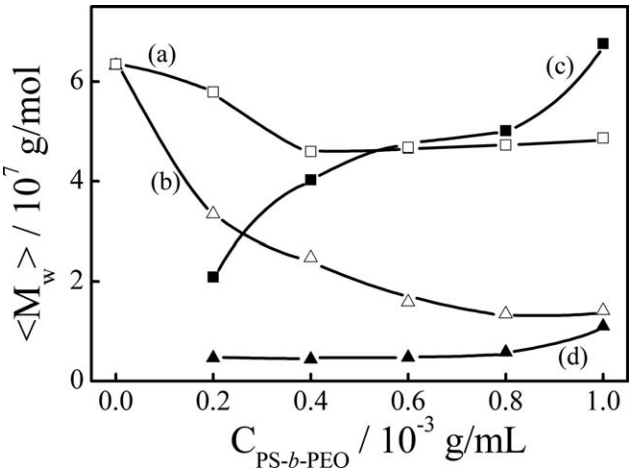

FIGURE 3 Initial PS-*b*-PEO concentration dependence on the average molar mass ($\langle M_w \rangle$) of the mixed micelles of PS-*b*-PEO and PS-*b*-PNIPAM or the pure micelles of PS-*b*-PEO, where all symbols have the same meanings as in Figure 1.

10^{-3} g/mL, which is because of the interchain association of PS-*b*-PEO with the concentration.

Figure 3 shows $C_{PS\text{-}b\text{-}PEO}$ dependence on the average molar mass $\langle M_w \rangle$ of the pure micelles and mixed micelles. For pure PS-*b*-PEO micelles, $\langle M_w \rangle$ increased with $C_{PS\text{-}b\text{-}PEO}$ due to the increase in the interchain association of diblock copolymers. For PS_{313}-*b*-PEO_{114}, the effect of the concentration on the $\langle M_w \rangle$ is larger because PS_{313}-*b*-PEO_{114} has a longer hydrophobic PS block. With the addition of PS_{313}-*b*-PEO_{114}, $\langle M_w \rangle$ of the mixed micelles decreased when the concentration of the PS_{313}-*b*-PEO_{114} increased from 0 to 6×10^{-4} g/mL and then leveled off with the increase in $C_{PS\text{-}b\text{-}PEO}$ from 6×10^{-4} g/mL to 1×10^{-3} g/mL. For PS_{108}-*b*-PEO_{114}, $\langle M_w \rangle$ decreases with the concentration in the range of 0 to 1×10^{-3} g/mL. To explain the decrease in the $\langle R_h \rangle$, $\langle R_g \rangle$, and $\langle M_w \rangle$ of the mixed micelles with the concentration of PS-*b*-PEO, we summarized the average aggregation number (N_{agg}) of the pure PS-*b*-PNIPAM micelles, pure PS-*b*-PEO micelles in Table 1. From Table 1, we know that for pure PS-*b*-PNIPAM micelles with $C_{PS\text{-}b\text{-}PNIPAM} = 1 \times 10^{-3}$ g/mL, N_{agg} is 1020, which is larger than the N_{agg} of pure PS_{108}-*b*-PEO_{114} micelles in its whole concentration region, indicating higher hydrophilic–hydrophobic ratio and less interchain association of PS_{108}-*b*-PEO_{114}. So to form stable mixed micelles, less PS_{108}-*b*-PEO_{114} diblock copolymer chains are needed to replace PS-*b*-PNIPAM copolymer chains. Furthermore, because of the replacement of PS-*b*-PNIPAM by PS_{108}-*b*-PEO_{114} in the mixed micelles, PNIPAM chains may shrink due to the decrease in the grafting density of the PNIPAM in the swollen shell, which makes the size smaller. Note that the $\langle M_w \rangle$ of PS_{108}-*b*-PEO_{114} (~16,200 g/mol) is much smaller than of PS-*b*-PNIPAM (~60,000 g/mol) causing the decrease in $\langle M_w \rangle$ of the mixed micelles. For PS_{313}-*b*-PEO_{114}, the situation is more complicated. From Table 1, we know its N_{agg} is 1800 is higher than N_{agg} of PS-*b*-PNIPAM when both of the initial concentrations were 1×10^{-3} g/mL, which means PS_{313}-*b*-PEO_{114} has a lower hydrophilic–hydrophobic ratio and higher interchain association. We have to realize that the $\langle M_w \rangle$ of PS_{313}-*b*-PEO_{114} is 37,600 g/mol which is smaller than $\langle M_w \rangle$ of PS-*b*-PNIPAM (~60,000 g/mol), which means that if one PS-*b*-PNIPAM diblock copolymer in each micelle is replaced by PS_{313}-*b*-PEO_{114}, the $\langle M_w \rangle$ still decreases. This is the reason for PS_{313}-*b*-PEO_{114} that $\langle R_h \rangle$, $\langle R_g \rangle$, and $\langle M_w \rangle$ decrease when its concentration is smaller than 6×10^{-4} g/mL. When the concentration of PS_{313}-*b*-PEO_{114} is higher than 6×10^{-4} g/mL, the effect of the initial concentration due to the interchain association offsets the effect of smaller $\langle M_w \rangle$, which holds the $\langle M_w \rangle$.

It is worth noting that Ding and coworker have reported that the phase transition temperature shifts to a lower temperature as the concentration of PEG increases by using ultrasensitive differential scanning calorimetry.[43] In our present experiments, PNIPAM blocks in the copolymer PS-*b*-PNIPAM and PEO chains were assumed to be confined in the swollen shell which made the local concentration of PEO chains higher. The higher concentration of PEO in the swollen shell may cause PNIPAM blocks further collapse which made the size of the mixed micelles smaller.

To look deep into the mixed micelles, we calculated the average number of the diblock copolymer PS-*b*-PEO ($\langle N_{PS\text{-}b\text{-}PEO} \rangle$) and the average diblock copolymer PS-*b*-PNIPAM in each mixed micelles ($\langle N_{PS\text{-}b\text{-}PNIPAM} \rangle$) from the $\langle M_w \rangle$ of the mixed micelles and the $\langle M_w \rangle$ of the PS-*b*-PEO and PS-*b*-PNIPAM diblock copolymers by assuming that the average composition of the mixed micelles is the same as that in the initial THF solution. The assumption is based on the facts that we did not observe any macroscopic precipitates in our experiments and the distribution of the hydrodynamic radius of the mixed micelles is very narrow. The fact that there were no precipitates indicates that all PS-*b*-PEO and PS-*b*-PNIPAM diblock copolymers chains in THF formed mixed micelles in the final solution, suggesting that the average composition of the mixed micelles should be as same as that in the initial THF solution. The narrow size distribution of the mixed micelles infers that the composition of the mixed micelles in final aqueous solution have a narrow distribution which makes the calculation meaningful, because if there exist mixed micelles with different composition far away from that in the initial mixture, i.e., with less or more PS-*b*-PNIPAM in the mixed micelles, the distribution of the mixed micelles will be rather wider due to the different chain lengths between PEO and PNIPAM. Figure 4 shows that the

TABLE 1 Average Aggregation Number (N_{agg}) of Pure PS-*b*-PEO Micelles and Pure PS-*b*-PNIPAM Micelle at 25 °C

	$C/10^{-3}$ (g/mL)				
Sample	0.2	0.4	0.6	0.8	1
PS_{108}-*b*-PEO_{114}	290	270	290	360	680
PS_{313}-*b*-PEO_{114}	560	1,070	1,240	1,330	1,800
PS-*b*-PNIPAM	–	–	–	–	1,020

hydrodynamic radius distribution of the pure PS_{108}-*b*-PEO_{114} micelles, mixed micelles, and pure PS-*b*-PNIPAM micelles, the respective peak of which are located at 23, 49, and 61 nm. The size distributions are narrow, which is reflected in the smaller values of the relative distribution width ($\mu_2/\langle\Gamma\rangle^2$). It clearly shows that the average hydrodynamic radius of PS_{108}-*b*-PEO_{114} is smaller than that of pure PS-*b*-PNIPAM due to the smaller initial concentration of PS_{108}-*b*-PEO_{114} in THF solution and higher hydrophilic–hydrophobic ratio of PS_{108}-*b*-PEO_{114}. With the addition of PS_{108}-*b*-PEO_{114}, the size of the mixed micelles decreased compared with that of pure PS-*b*-PNIPAM. There is no peak near that of the pure PS-*b*-PEO micelles, indicating that only mixed micelles exist without pure PS-*b*-PEO micelles in the solution. Note that the size distribution of pure PS-*b*-PNIPAM micelles is relatively broader, which may be due to the relatively broader distribution of the PS_{207}-*b*-$PNIPAM_{357}$ diblock copolymer as well as the nonuniformity of the PNIPAM chains in the corona of the pure PS-*b*-PNIPAM micelles.

Figure 5 indicates that for both PS_{313}-*b*-PEO_{114} and PS_{108}-*b*-PEO_{114} diblock copolymers, the average aggregation number of PS-*b*-PNIPAM $\langle N_{\text{PS-}b\text{-PNIPAM}}\rangle$ decreased with the concentration of PS-*b*-PEO. Note that when $C_{\text{PS-}b\text{-PEO}} = 0$, the average number of PS-*b*-PEO ($\langle N_{\text{PS-}b\text{-PEO}}\rangle$) in the micelles equals to 0. The average aggregation number of PS_{108}-*b*-PEO_{114} increased to a maximum ~400 and was kept as a constant with the further increase in the concentration of PS_{108}-*b*-PEO_{114}. While the average aggregation number of PS_{313}-*b*-PEO_{114} increased with the concentration up to 1×10^{-3} g/mL. The change of the aggregation number of the diblock copolymer in each mixed micelles further gave us a clear image about the decrease in the size of the mixed micelles because the aggregation number of the PS-*b*-PNIPAM in each mixed micelles decreased.

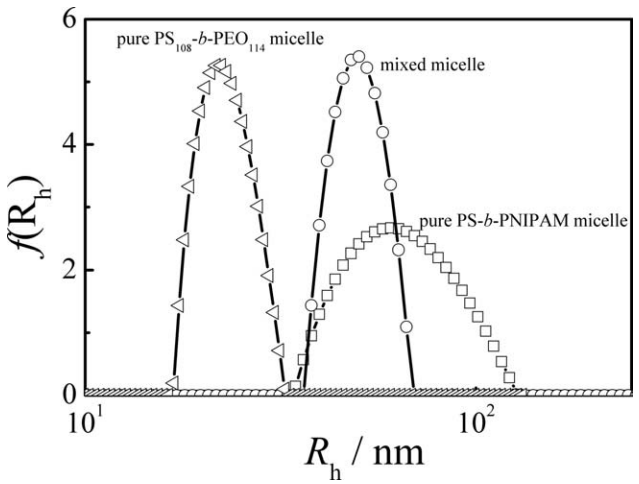

FIGURE 4 Hydrodynamic radius distribution of the pure PS_{108}-*b*-PEO_{114} micelles, the pure PS-*b*-PNIPAM micelles, and the mixed micelles of PS_{108}-*b*-PEO_{114} and PS-*b*-PNIPAM, where the initial concentration of PS_{108}-*b*-PEO_{114} for pure PS-*b*-PEO micelles and the initial concentration of PS-*b*-PNIPAM for pure PS-*b*-PNIPAM were 2×10^{-4} g/mL and 1×10^{-3} g/mL, respectively. The initial concentrations of PS_{108}-*b*-PEO_{114} and PS-*b*-PNIPAM for mixed micelles were the same as that for pure micelles.

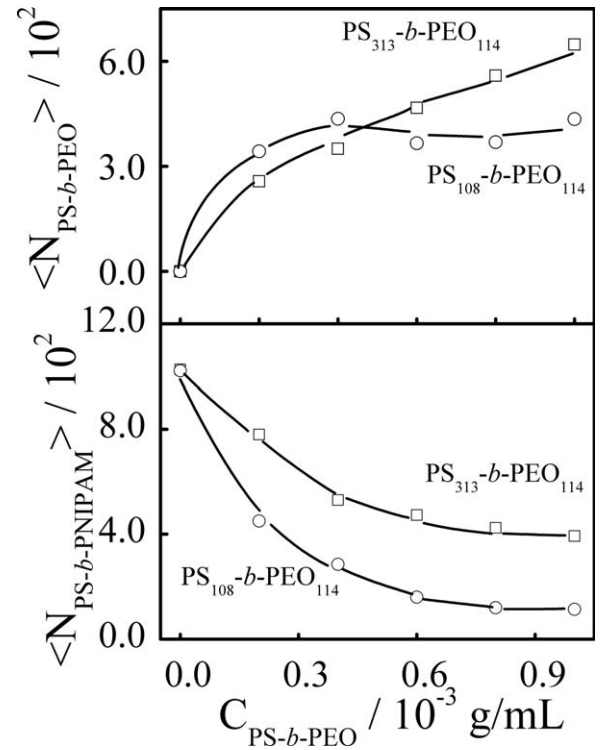

FIGURE 5 Initial PS-*b*-PEO concentration dependence on the average aggregation number of PS-*b*-PEO ($\langle N_{\text{PS-}b\text{-PEO}}\rangle$) and the average aggregation number of PS-*b*-PNIPAM ($\langle N_{\text{PS-}b\text{-PNIPAM}}\rangle$) in each mixed micelle.

Figure 6 reveals that in each mixed micelles, the N_{total} is kept as a constant with the concentration of PS_{313}-*b*-PEO_{114}, whereas the N_{total} decreased with the concentration of the PS_{108}-*b*-PEO_{114}. The different influence on the total aggregation number of the mixed micelles could be attributed to the

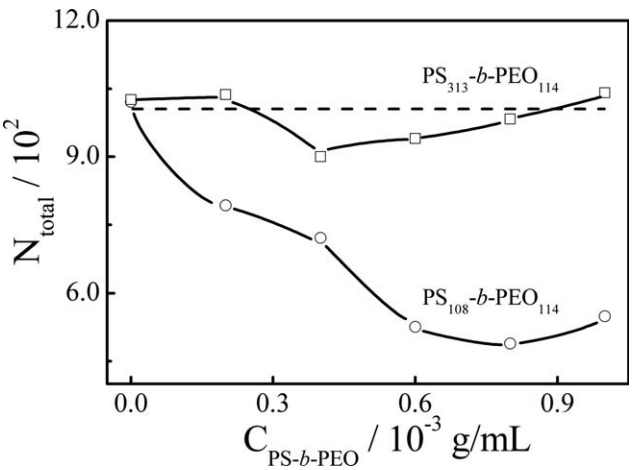

FIGURE 6 Total average aggregation number of the diblock copolymer PS-*b*-PEO and PS-*b*-PNIPAM (N_{total}) in each mixed micelle versus the concentration of PS-*b*-PEO, where the initial concentration of PS-*b*-PNIPAM in THF was 1×10^{-3} g/mL.

difference between the hydrophilic–hydrophobic ratio of the PS-*b*-PNIPAM and that of the PS-*b*-PEO. Figure 7 shows with the addition of PS_{313}-*b*-PEO_{114}, the decrease in $\langle R_h \rangle$ and $\langle R_g \rangle$ of the mixed micelles with the temperature becomes much more gradually, which is consistent with the results reported by Ding et al.,[43] i.e., by using ultrasensitive differential scanning calorimetry, they found that with the addition of PEO, the transition of PNIPAM has become wider. Figure 8 schematically summarized the self-assembly of the pure PS-*b*-PNIPAM and mixed micelles of PS-*b*-PNIPAM and PS-*b*-PEO and the shrinkage of the PNIPAM blocks.

CONCLUSIONS

Two narrowly distributed PS-*b*-PEO diblock copolymer with the same PEO block and different PS blocks and amphiphilic diblock copolymer PS-*b*-PNIPAM were synthesized by ATPR and RAFT, respectively. Mixed micelles of PS-*b*-PEO and PS-*b*-PNIPAM were prepared by a microphase inversion. The study of the PS-*b*-PEO concentration dependence on the size and average molecular weight of the mixed micelles by using a combination of static and dynamic laser light scattering reveals that the size and average molecular weight of the mixed micelles decreased due to the difference between the hydrophilic–hydrophobic ratio of PS-*b*-PEO and PS-*b*-PNIPAM as well as the decrease in the grafting density of the PNIPAM chains in the swollen shells.

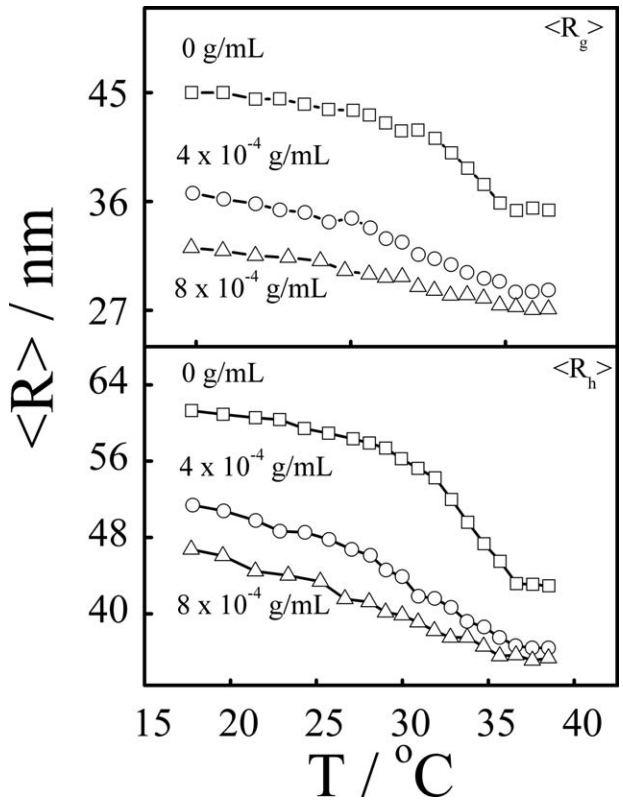

FIGURE 7 Temperature dependence on the average hydrodynamic radius $\langle R_h \rangle$ and $\langle R_g \rangle$ of the pure PS-*b*-PNIPAM micelle and the mixed micelles with two different amounts of PS_{313}-*b*-PEO_{114} ($C_{PS\text{-}b\text{-}PEO} = 4 \times 10^{-4}$ g/mL or 8×10^{-4} g/mL), where the initial concentration of PS-*b*-PNIPAM in THF was 1×10^{-3} g/mL.

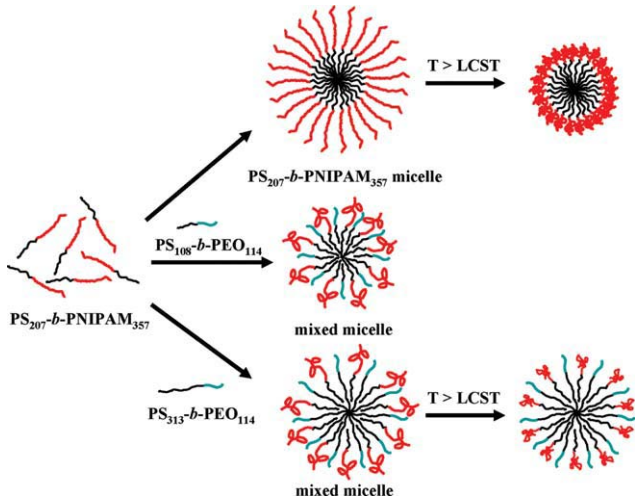

FIGURE 8 Schematic of the self-assembly of the pure PS-*b*-PNIPAM micelles, mixed micelles of PS-*b*-PEO and PS-*b*-PNIPAM and the shrinkage of PNIPAM blocks.

The authors thank Professor Guangzhao Zhang and Dr. Xuechang Zhou for the donation of the PS-*b*-PNIPAM sample and for their valuable comments about the manuscript. The financial support of the National Natural Scientific Foundation of China (NNSFC) Projects to (20804043), Specialized Research Fund for the Doctoral Program of Higher Education (200803581022) and Chinese Universities Scientific Fund is gratefully acknowledged.

REFERENCES AND NOTES

1 Spatz, J. P.; Roescher, A.; Möller, M. Adv Mater 1996, 8, 337–340.

2 Corcos, F.; Bourgeat-Lami, E.; Novat, C.; Lang, J. Colloid Polym Sci 1999, 227, 1142–1151.

3 Han, K.; Miah, M. A. J.; Shanmugam, S.; Yong, C. S.; Choi, H. G.; Kim, J. A.; Yoo, B. K. Arch Pharm Res 2007, 30, 1344–1349.

4 Xu, R. L.; Winnik, M. A.; Hallet, F. R.; Riess, G.; Croucher, M. D. Macromolecules 1991, 24, 87–93.

5 Bronstein, L. M.; Chernyshov, D. M.; Timofeeva, G. I.; Dubrovina, L. V.; Valetsky, P. M.; Khokhlov, A. R. Langmuir 1999, 15, 6195–6200.

6 Mortensen, K.; Brown, W.; Almdal, K.; Alami, E.; Jada, A. Langmuir 1997, 13, 3635–3645.

7 Wang, Y. M.; Mausch, C. M.; Chun, M.; Quirk, R. P.; Mattice, W. L. Macromolecules 1995, 28, 904–911.

8 Zhao, C. L.; Winnik, M. A.; Riess, G.; Croucher, M. D. Langmuir 1990, 6, 514–516.

9 Wilhelm, M.; Zhao, C. L.; Wang, Y. C.; Xu, R. L.; Winnik, M. A.; Mura, J. L.; Riess, G.; Croucher, M. D. Macromolecules 1991, 24, 1033–1040.

10 Caldérara, F.; Hruska, Z.; Hurtrez, G.; Lerch, J. P.; Nugay, L. T.; Riess, G. Macromolecules 1994, 27, 1210–1215.

11 Yu, K.; Zhang, L. F.; Eisenberg, A. Langmuir 1996, 12, 5980–5984.

12 Yu, K.; Eisenberg, A. Macromolecules 1996, 29, 6359–6361.

13 Yu, K.; Eisenberg, A. Macromolecules 1998, 31, 3509–3518.

14 Bronstein, L. M.; Chernyshov, D. M.; Timofeeva, G. I.; Dubrovina, L. V.; Valetsky, P. M.; Khokhlov, A. R. J Colloid Interface Sci 2000, 230, 140–149.

15 Bronstein, L. M.; Chernyshov, D. M.; Timofeeva, G. I.; Dubrovina, L. V.; Valetsky, P. M.; Obolonkova, E. S.; Khokhlov, A. R. Langmuir 2000, 16, 3626–3632.

16 Bronstein, L. M.; Chernyshov, D. M.; Vorontsov, E.; Timofeeva, G. I.; Dubrovina, L. V.; Valetsky, P. M.; Kazakov, S.; Khokhlov, A. R. J Phys Chem B 2001, 105, 9077–9082.

17 Rangelov, S.; Dimitrov, P.; Tsvetanov, C. B. J Phys Chem B 2005, 109, 1162–1167.

18 Zhao, F.; Xie, D. H.; Zhang, G. Z.; Pispas, S. J Phys Chem B 2009, 112, 6358–6362.

19 Pispas, S.; Sarantopoulou, E. Langmuir 2007, 23, 7484–7490.

20 Zhao, J. P.; Zhang, G. Z.; Pispas, S. J Phys Chem B 2009, 113, 10600–10606.

21 Cho, C. S.; Cheon, J. B.; Jeong, Y. I.; Kim, I. S.; Kim, S. H.; Akaike, T. Macromol Rapid Commun 1997, 18, 361–369.

22 Cho, C. S. Polymer 1999, 40, 2041–2050.

23 Nuopponen, M.; Ojala, J.; Tenhu, H. Polymer 2004, 45, 3643–3650.

24 Tang, T.; Castelleto, V.; Parras, P.; Hamley, I. W.; King, S. M.; Roy, D.; Perrier, S.; Hoogenboom, R.; Schubert, U. S. Macromol Chem Phys 2006, 207, 1718–1726.

25 Zhang, W. A.; Zhou, X. C.; Li, H.; Fang, Y. E.; Zhang, G. Z. Macromolecules 2005, 38, 909–914.

26 Yan, Y. F.; Zhou, X. C.; Ji, J.; Yan, L. F.; Zhang, G. Z. J Phys Chem B 2006, 110, 21055–21059.

27 Wu, C.; Zhou, S. Q. Macromolecules 1995, 28, 8381–8387.

28 Hu, T. J.; You, Y. Z.; Pan, C. Y.; Wu, C. J Phys Chem B 2002, 106, 6659–6662.

29 Tian, M. M.; Qin, A. W.; Ramireddy, C.; Webber, S. E.; Munk, P. Langmuir 1993, 9, 1741–1748.

30 Shan, J.; Chen, J.; Nuopponen, M.; Tenhu, H. Langmuir 2004, 20, 4671–4676.

31 (a) Thang, S. H.; Chong, Y. K.; Mayadunne, R. T. A.; Moad, G.; Rizzardo, E. Tetrahedron Lett 1999, 40, 2435–2438; (b) Goto, A.; Sato, K.; Tsujii, Y.; Fukuda, T.; Moad, G.; Rizzardo, E.; Thang, S. H. Macromolecules 2001, 34, 402–408.

32 Zhang, H. L.; Sun, X. Y.; Wang, X. Y.; Zhou, Q. F. Macromol Rapid Commun 2005, 26, 407–411.

33 Zhao, Y.; Liang, H. J.; Wang, S. G.; Wu, C. J Phys Chem B 2001, 105, 848–851.

34 Liu, S. Y.; Hu, T. J.; Liang, H. J.; Jiang, M.; Wu, C. Macromolecules 2000, 33, 8640–8643.

35 Zhang, G. Z.; Liu, L.; Zhao, Y.; Ning, F. L.; Jiang, M.; Wu, C. Macromolecules 2000, 33, 6340–6343.

36 Zimm, B. H. J Chem Phys 1948, 16, 1099–1115.

37 Chu, B. Laser Light Scattering, 2nd ed.; Academic Press: New York, 1991.

38 Xia, J.; Dubin, P. In Macromolecular Complexes in Chemistry and Biology; Dubin, P.; Bock, J.; Davies, R. M.; Schultz, D. N.; Thies, C., Eds.; Spring-Verlag: New York, 1994; p 247.

39 Berne, B.; Pecora, R. Dynamic Light Scattering; Plenum Press: New York, 1976.

40 Provercher, S. W. J Chem Phys 1978, 69, 4273–4276.

41 Provercher, S. W. Makromol Chem 1979, 180, 201–209.

42 Burchard, W. In Light Scattering. Principles and Development; Brown, W., Ed.; Oxford University Press: Oxford, UK, 1996; pp 439–476.

43 Ding, Y. W.; Zhang, G. Z. J Phys Chem C 2007, 111, 5309–5312.